



Cadmium–Aluminum Layered Double Hydroxide Microspheres for Photocatalytic CO₂ Reduction

Daniel Saliba,^[a] Alaa Ezzeddine,^[b] Rachid Sougrat,^[c] Niveen M. Khashab,^[b] Mohamad Hmadeh,^{*[a]} and Mazen Al-Ghoul^{*[a]}

We report the synthesis of cadmium–aluminum layered double hydroxide (CdAl LDH) using the reaction-diffusion framework. As the hydroxide anions diffuse into an agar gel matrix containing the mixture of aluminum and cadmium salts at a given ratio, they react to give the LDH. The LDH self-assembles inside the pores of the gel matrix into a unique spherical-porous shaped microstructure. The internal and external mor-

phologies of the particles are studied by electron microscopy and tomography revealing interconnected channels and a high surface area. This material is shown to exhibit a promising performance in the photoreduction of carbon dioxide using solar light. Moreover, the palladium-decorated version shows a significant improvement in its reduction potential at room temperature.

Introduction

Layered double hydroxides (LDH) are widely used as catalysts and catalysts precursors.^[1–3] LDHs are anionic layered clays whose crystal structure is based on that of the brucite [M^{II}(OH)₂] where the divalent metal cations (M^{II}) are octahedrally surrounded by hydroxyl groups that share edges to form infinite 2D neutral sheets.^[4] The partial substitution of some divalent metal cations by trivalent ones generates an excess in the positive charges on the brucite-like sheets leading to the intercalation of some charge-balancing anions in the interlayer region.^[5,6] LDHs are generally expressed by the following formula [M^{II}_{1-x}M^{III}_x(OH)₂]^{x+}(Aⁿ⁻)_{x/n}·yH₂O, where M^{II} and M^{III} are the divalent and the trivalent metal cations, respectively. Aⁿ⁻ is the charge balancing anion and *x* is the cationic ratio [M^{III}/(M^{II} + M^{III})].^[7] To form a stable LDH structure, M^{II} and M^{III} metal cations should have ionic radii ranging from 65 to 89 pm and from 62 to 69 pm, respectively.^[6] In recent years, the rapid development of molecular dynamics (MD) computer simulations of LDH materials shed light into the structure and arrangement of various molecules and ions in the interlayers and their dy-

namics (i.e., intercalation and deintercalation), and played a crucial role in unraveling the intricate interplay between LDH structure, energetics, and reactivity.^[8–11]

LDHs are materials with surface, interlayer, and electronic properties that render them a compelling choice as photocatalysts.^[12] Some LDHs were shown to exhibit photocatalytic activity for the degradation of organic compounds,^[13] oxygen or hydrogen gas evolution from water,^[14] and carbon dioxide reduction in the presence of water or hydrogen gas.^[15,16] Specifically, the presence of an interlayer spacing plays a major role in increasing the sorption capacity of carbon dioxide that intercalates and binds to the hydroxyl groups to form hydrogen carbonate intermediates.^[12] Thus, upon light irradiation, the metals in the LDH sheets facilitate charge separation and the hydrogen carbonate intermediates are reduced.^[15,16]

While cadmium cations (*r*_{Cd} = 109 pm) are reported to be incompatible with the formation of stable brucite-like layers,^[4] in this work we present the synthesis of stable cadmium–aluminum (CdAl) LDH using a reaction-diffusion framework where a sodium hydroxide solution (outer electrolyte) is added on top of an agar gel matrix containing the Cd²⁺/Al³⁺ mixture (inner electrolytes) at a given cationic ratio (Figure 1). Upon addition of the outer electrolyte, a supersaturation gradient is generated along the tube (reactor) starting at the outer/gel interface and ending at the gel/solid interface. The role of the gel is crucial in this framework as it eliminates both convection currents and sedimentation of the solids that nucleate, grow, and self-assemble in its pores.^[17,18] The gel also inhibits the rate of nucleation and growth, which might affect positively the crystallinity of the solid as well as the self-assembly of building units into organized and complex structures. This novel method of synthesis is thus based on interplay between reaction, diffusion, slow nucleation, and crystal growth. It is beneficial for many reasons: 1) it allows the stabilization of the unstable CdAl LDH inside the pores of the gel even after ex-

[a] D. Saliba, Prof. M. Hmadeh, Prof. M. Al-Ghoul
Department of Chemistry
American University of Beirut
P.O.Box 11-0236, Riad El-Solh 1107 2020, Beirut (Lebanon)
Fax: (+961) (1)365217
E-mail: mohamad.hmadeh@aub.edu.lb
mazen.ghoul@aub.edu.lb

[b] Dr. A. Ezzeddine, Prof. N. M. Khashab
Smart Hybrid Materials (SHMs) Lab
King Abdullah University of Science and Technology (KAUST)
Thuwal 23955-6900 (Kingdom of Saudi Arabia)

[c] Dr. R. Sougrat
Imaging and Characterization Core Lab
King Abdullah University of Science and Technology (KAUST)
Thuwal 23955-6900 (Kingdom of Saudi Arabia)

Supporting Information for this article can be found under <http://dx.doi.org/10.1002/cssc.201600088>.

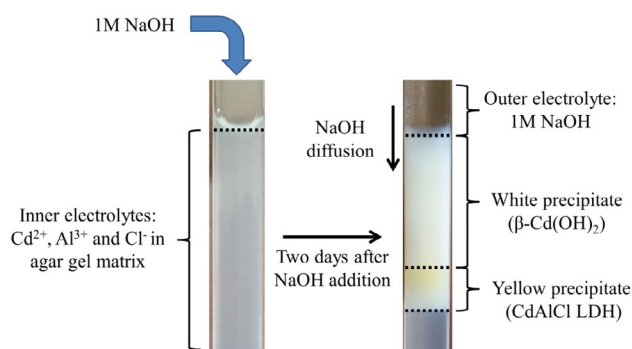


Figure 1. Schematic representation of the co-synthesis of the CdAl LDH (yellow band) and the β -Cd(OH)₂ crystals (white band).

traction of the solid; 2) it is carried out under facile conditions compared to the well-known co-precipitation method where control of the pH, thermal treatment, and aging of the LDH are required,^[4,19] and 3) it confines the self-assembly of the CdAl LDH into a unique spherical-porous shaped microstructure, which is difficult to obtain using the other preparation methods. For example, the co-precipitation method generally yields platelet morphologies owing to the preferential growth of the brucite sheets (perpendicular to the stacking direction).^[20,21] The obtained spherical morphology is of major interest for a number of applications, mainly in catalysis.^[20]

Results and Discussion

The extracted yellow precipitate (CdAl LDH) is characterized using a range of spectroscopic techniques. Electron microscopy and tomography are applied to investigate the morphology of the particles. Finally, the solar powered photocatalytic carbon dioxide reduction over CdAl LDH and palladium-decorated CdAl LDH nanostructures are examined.

Powder X-ray diffraction

The powder XRD diffraction pattern of the yellow band (Figure 2A) presents six sharp peaks at around 11° (003), 22° (006), 34° (009), 38° (015), 60° (110), and 62° (113), revealing its nature as being LDH with a rhombohedral symmetry.^[5] The corresponding lattice parameter c is calculated from

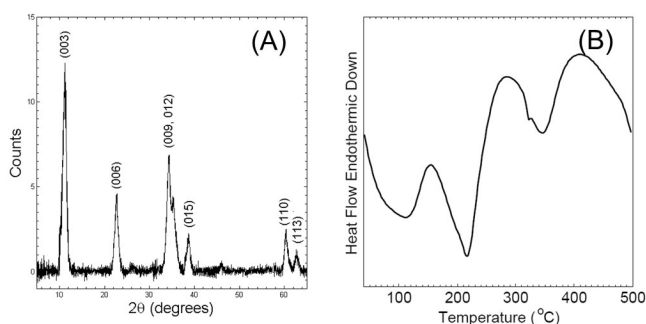


Figure 2. (A) Powder XRD pattern and (B) DSC spectrum of the CdAl LDH.

Bragg's equation and is found to be $c = 23.5 \text{ \AA}$, whereas the other lattice parameter a is equal to 3.2 \AA .

Differential scanning calorimetry

The differential scanning calorimetry (DSC) of the synthesized CdAl LDH (Figure 2B) presents three endothermic peaks. The first one (60–140 °C) is attributed to the loss of both adsorbed and interlayer water, whereas the second (210 °C) corresponds to the Cd–OH de-hydroxylation and the final heat flow, at around 335 °C, is ascribed to the Al–OH de-hydroxylation. The shoulder at 315 °C is attributed to the loss of the interlayer carbonates (de-carbonation).^[22]

Solid-state ²⁷Al NMR

The solid-state ²⁷Al NMR spectrum (Figure S1 in the Supporting Information) of the CdAl LDH shows one peak at a chemical shift around 15 ppm, which proves the octahedral coordination of all the aluminum elements in the brucite-like sheets of the LDH, as the range of the octahedral coordination (Al_{octa}) is 0–20 ppm.^[23]

UV/Vis diffuse reflectance

The synthesized CdAl LDH exhibits a wide absorption band ranging from the near UV (210 nm) to the visible region (650 nm) of the electromagnetic spectrum. Figure S2 shows the UV/Vis diffuse reflectance spectrum of the CdAl LDH where three main absorption bands are centered at around 225, 276, and 360 nm. The obtained reflectance data is transformed into the Kubelka–Munk model.

Scanning electron imaging and elemental mapping

Figure 3A–B shows typical SEM images of the synthesized LDH, which indicate the self-assembly of the CdAl LDH into microspheres having flowery-like structures with diameters ranging from 4 to 11 μm. Further examination of these spheres indicates that the material consists of packed nano-sheets that are curved and connected to each other to form this flowery-like porous structure. Even after ultra-sonication of a suspension of this material for 8 h, the SEM image (Figure S3A) shows that the shape of the particles remains the same. Moreover, the calcination of the LDH at 500 °C in nitrogen atmosphere for 3 h leads to a collapse of the pores (Figure S3B), yet the spherical shape is maintained. Accordingly, both the calcination and ultra-sonication indicate that the nano-sheets are strongly connected to each other. Elemental mapping reveals the homogeneous distribution of the aluminum (Figure 3C) and cadmium (Figure 3D) over the particle surface.

Electron tomography

TEM imaging and 3D electron tomography are performed for further investigation of the internal structure of the CdAl particles. Figure 4A illustrates a typical TEM image of the material

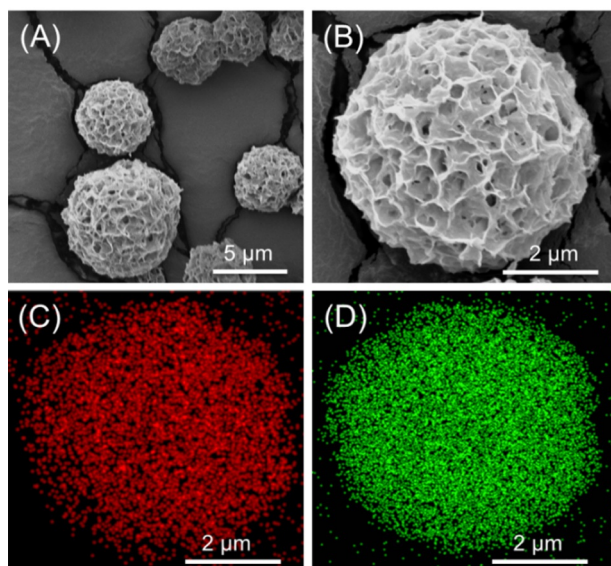


Figure 3. (A, B) SEM images of the CdAl LDH and element mapping of (C) aluminum and (D) cadmium using EDX on SEM.

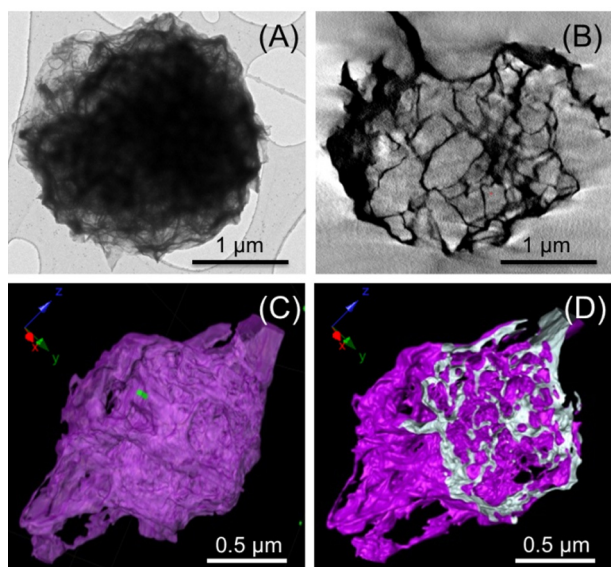


Figure 4. (A) TEM image, (B) 2D virtual cross-sectional slice, (C) 3D tomographic reconstruction, and (D) cross-sectional cut showing the internal microstructure of the CdAl LDH.

in addition to a virtual cross-sectional cut (Figure 4B) along the particle. This cut reveals the internal structure that consists of many individual nano-sheets having an average thickness of 30 nm and connected to each other to create channels and void. A 3D reconstruction of the flower-like structure is shown in Figure 4C along with a cross sectional cut throughout the (*x*-*y*) plane proving the void presence inside the structure (white color in Figure 4D).

Textural properties

The textural properties and optimal surface area of the synthesized CdAl LDH are studied by means of nitrogen Brunauer–

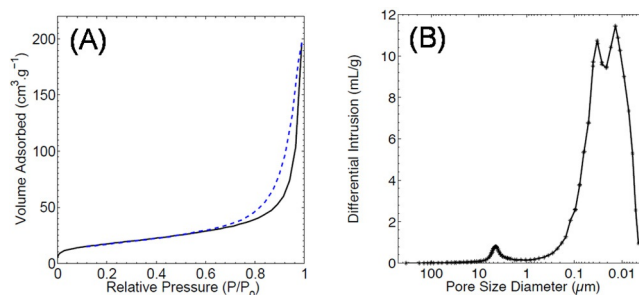


Figure 5. (A) Nitrogen adsorption (—) and desorption (----) isotherms and (B) pore size distribution of the CdAl LDH.

Emmett–Teller (BET) and mercury porosimetry. The nitrogen adsorption and desorption isotherms (Figure 5A) can be assigned as a type IV isotherm with a hysteresis loop of type H3. The sample illustrates a wide pore-size distribution located across the range of 5–110 nm, which matches the hysteresis loop of type H3 as it is characteristic for solids with wide pore-size distribution.^[24] Nevertheless, nitrogen adsorption/desorption shows a major drawback as it is only applicable to solids with pore size ranging from 1.8 to 300 nm,^[25] however, the mercury porosimetry measurement (Figure 5B) shows another pore-size distribution in the range between 3 and 6 μm, which is located outside the detection limit of the nitrogen adsorption/desorption method. These large pores are a result of the large void in the internal structure of the CdAl LDH. The computed surface area is 116 m²g⁻¹ with a pore volume of 0.31 cm³g⁻¹ and a bulk density of 0.162 g mL⁻¹. Upon calcination, the surface area and the pore volume decrease to a value of 11 m²g⁻¹ and 0.025 cm³g⁻¹, respectively, indicating the total collapse of the pores and the internal structure as seen in the SEM image (Figure S2B).

Applications

Its unique spherical hierarchical morphology, relatively high surface area, absorption of the visible light, and the fact that an LDH surface has an abundance of OH groups that increase the material's affinity toward carbon dioxide molecules make the obtained CdAl LDH compatible in the photoreduction of carbon dioxide using solar light. The first step in the photocatalytic conversion of carbon dioxide is the adsorption of the carbon dioxide molecules on the surface or within the photocatalyst, followed by activation under irradiation. To this end, the affinity of CdAl LDH toward carbon dioxide molecules was monitored via TGA at room temperature (RT) in the presence of a continuous flow of carbon dioxide (Figure S4). A weight increase of 0.088% was observed corresponding to 0.2 mmol g⁻¹. The photocatalytic carbon dioxide reduction reaction was then performed in a gas phase batch reactor in the presence of hydrogen (see Experimental Section for more details).^[26] ¹³C₂O₂ isotope labeling experiments were subsequently performed to prove the carbon source of the products originated from carbon dioxide as opposed to adventitious carbon contamination on the sample.^[27] The reaction was performed

at two different temperatures (RT and 100 °C) both in the presence and absence of irradiation. At RT, a significant amount of ^{12}CO (214 $\text{nmol g}^{-1} \text{h}^{-1}$) and a negligible concentration of $^{12}\text{CH}_4$ (4 $\text{nmol g}^{-1} \text{h}^{-1}$) were detected (Figure S5). In the second run, we observed a decrease in the concentration of the detected products (161 and 2 $\text{nmol g}^{-1} \text{h}^{-1}$ of ^{12}CO and $^{12}\text{CH}_4$, respectively; Figure S5). This result indicates that the detected products at RT originate from the carbon residue on the catalyst surface. Interestingly, at 100 °C and under irradiation, a small amount of ^{13}CO (29 u) was observed (26 $\text{nmol g}^{-1} \text{h}^{-1}$, Figure S6). It is noted that a negligible amount of product was detected in absence of light, which indicated that the carbon dioxide to carbon monoxide conversion is a light-driven process. After the initial first run, the light yellow color of the sample transformed to dark brown suggesting that the CdAl LDH is unstable under the reaction conditions. This was further confirmed by powder XRD analysis (Figure 6E). Moreover, no products were observed after the second run, demonstrating that the structural changes to the CdAl LDH resulted in the deactivation of the material under the operating experimental conditions (100 °C in the presence of hydrogen gas).^[28] To use our catalyst at RT, palladium nanoparticles were employed as co-catalysts.^[29] To this end, heteronanostructures of Pd–CdAl LDHs were prepared (0.5 wt% CdAl LDH) and the obtained material was examined at RT. The palladium nanoparticles (NPs) were previously prepared through several different methods (colloidal synthesis, hydrothermal synthesis, and microwave assisted). However, there are relatively few examples of microwave-assisted synthesis employed in the preparation of supported metal particles.^[30] To prepare our Pd–CdAl LDHs heteronanostructures, a microwave assisted solvothermal technique, using

ethanol as a reducing agent, was successfully carried out (more details can be found in the Experimental Section). Owing to the low metal loading (0.5 wt%) and the small diameter of the nanoparticles (3–7 nm), there are no powder XRD diffraction peaks associated with the palladium NPs. However, the palladium NPs are clearly seen in the SEM images (Figure S7A, B). The palladium NPs were found to be single crystals and well dispersed on the surface, with diameters ranging from 3 to 7 nm (Figure S7B). The HRTEM images show atomic planes with spacing of 0.23 and 0.14 nm for the NPs (Figure 6A–D). These are ascribed to the (111) and (022) reflection planes of bulk palladium, respectively. The photocatalytic activity of the as-synthesized heteronanostructures was evaluated at RT under identical conditions employed for the pure CdAl LDH. Interestingly, a ^{13}CO product (29 u, Figure S8) was detected and the rate was calculated to be 64 $\text{nmol g}^{-1} \text{h}^{-1}$. This measurement was repeated multiple times for several runs (3 runs, 17 h of irradiation per run; Figure 6F). These results demonstrate that the Pd–CdAl LDHs are capable of converting gaseous carbon dioxide to carbon monoxide photocatalytically. The powder XRD pattern of the sample conclusively proves that the CdAl LDH structure is maintained throughout the photocatalytic reaction (Figure 6E). These measurements also demonstrate that Pd–CdAl LDH is stable under these reaction conditions and the results are reproducible even after being irradiated continuously for 4 days.

Conclusions

We synthesized, stabilized, and fully characterized cadmium–aluminum layered double hydroxide (CdAl LDH) using a reac-

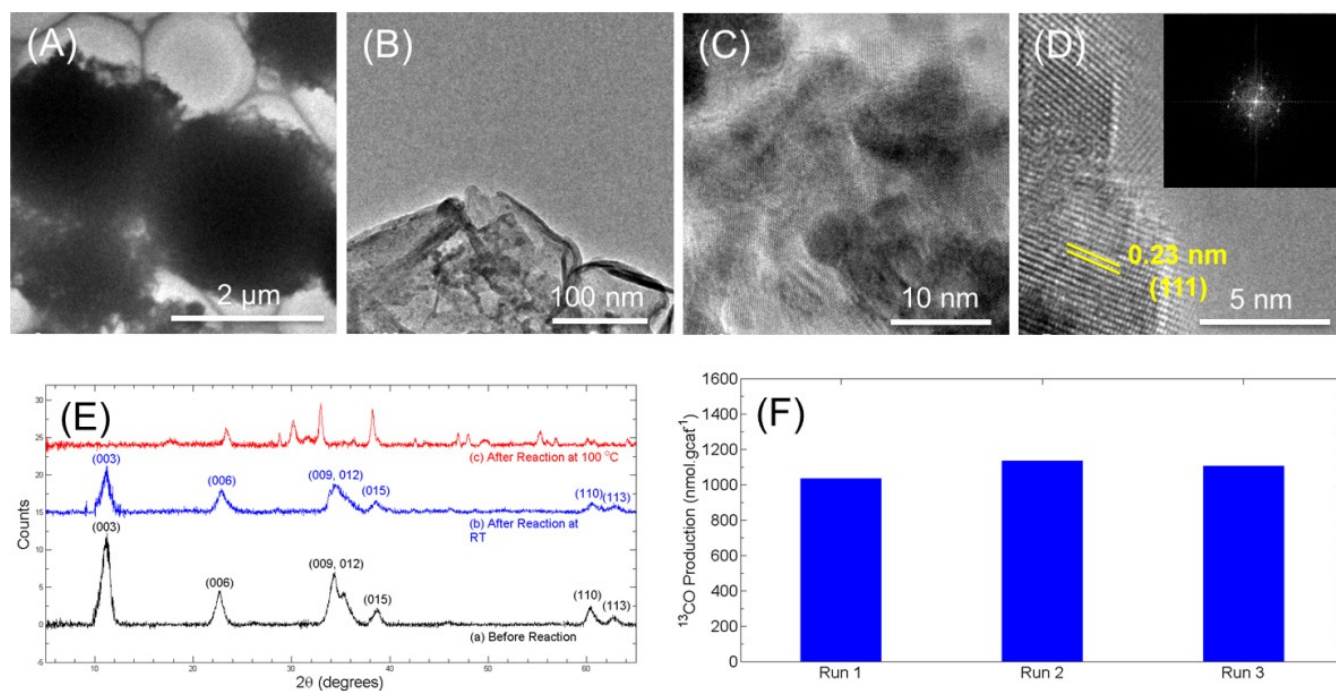


Figure 6. (A) HRTEM image; (B, C) magnification of image A; (D) diffraction planes of the palladium particles; (E) powder XRD of the LDH (a) before reaction, (b) after reaction at RT, and (c) after reaction at 100 °C; and (F) the ^{13}CO production rate for three consecutive runs (17 h per run).

tion-diffusion framework with agar gel as a matrix where precipitation reaction took place. The interplay of reaction and diffusion with slow nucleation and growth inside the pores of the gel provided stable porous spherical particles of LDH. High resolution TEM and electron tomography were used to characterize the internal structure of the particles and revealed an interesting pore-channel topology. The material was then tested for photocatalytic activity to reduce carbon dioxide under solar irradiation. Whereas the material showed activity in that regard, the palladium-decorated version showed a noticeable improvement.

Experimental Section

Materials

Cadmium chloride, aluminum chloride, and sodium hydroxide pellets were provided by Sigma-Aldrich. Agar was supplied by Invitrogen. All the chemicals were directly used without any purification.

Preparation method

Stock solutions of cadmium chloride and aluminum chloride, having a concentration of 0.75 M and 0.25 M for CdCl₂ and AlCl₃, respectively ($x=1/4$), were prepared using de-ionized water. After addition of 1% w/w of agar gel, the mixture was heated (~90 °C) and stirred until total dissolution of the gel. Then, the total mixture was poured into a test tube and left for 2 h to polymerize at ambient temperature. After gelling, the outer electrolyte (1 M of NaOH) was added on top of the gel. Two days after diffusion of the hydroxide anions through the gel matrix, two colored precipitates were formed, the yellow precipitate (CdAl LDH) followed by a white one [β -Cd(OH)₂, Figure 1]. The yellow band was extracted and washed with water under continuous heating (~90 °C) and stirring to redissolve the entire gel network. Finally, the solid was separated from the solution by centrifugation and freeze dried for 10 h. The empirical formula was established using TGA and energy dispersive X-ray spectroscopy (EDX) and found to be Cd_{0.75}Al_{0.25}(OH)₂(Cl)_{0.19}(CO₃)_{0.03}·0.4H₂O.

Nanostructured palladium LDHs were synthesized using a microwave-assisted reaction. Typically, 50 mg of LDH microspheres were suspended in anhydrous ethanol (15 mL) in a Pyrex vessel. A stock solution (1 mg mL⁻¹) of Na₂PdCl₄·3H₂O (Alfa Aesar) was prepared in anhydrous ethanol. An adequate volume of palladium solution was added to the dispersion of 50 mg LDHs in ethanol under sonication. After 30 min of sonication, the vessel was capped and transferred to the microwave reactor (CEM Discover, 200 W, 220 psi = 1.5 MPa, 150 °C, 30 min). After filtration and washing with deionized water, the sample was placed into a vacuum oven at 50 °C for 24 h.

Solid characterization

The powder XRD patterns were recorded by a Bruker D8 Advance XRD diffractometer using Cu_{K α} radiation ($\lambda = 1.5406 \text{ \AA}$). The accelerating voltage was set at 40 mA and 35 kV, at a scanning rate of 4° min⁻¹ and a step size of 0.02 s. The thermal behavior of the product was studied using a differential scanning calorimeter (DSC 204 F1 Phoenix, Netzsch, Germany). The heating rate was set to 10 °C min⁻¹ under nitrogen atmosphere with a flow rate of 40 mL min⁻¹. The 1D solid-state ²⁷Al NMR spectrum was recorded

at a resonance frequency of 104.27 MHz by collecting 1024 transients with 2 s recycle delay with 12000 spinning rate using a double resonance broadband BB¹H 4 mm Bruker cross polarization magic angle spinning (CP/MAS) probe. The mercury porosimetry measurement was carried out with an Auto Pore IV 9500 apparatus from Micromeritics, USA. Nitrogen adsorption/desorption isotherms were measured using a Micromeritics ASAP 2420 analyzer. The diffuse reflectance experiment was performed on a JASCO V-570 UV/Vis/NIR spectrophotometer. The CdAl particles were imaged using Titan CT (FEI Company) operating at 300 kV equipped with a 4k×4k CCD camera (Gatan). Tilt series for tomographic reconstruction were acquired using the Xplore 3D tomography software (FEI Company). The sample was tilted typically from -65° to +65°. Images were captured at 2° intervals between 0° and 50° and every single degree between 50° and 65°. Tilts series were aligned and tomograms were generated using IMOD.^[31,32] 3D rendering models were generated with the segmentation tools implemented in Avizo. The morphology of the samples was conducted on a Nova Nano 630 FEG from FEI with a through-the-lens detector (TLD). For gas-phase photocatalytic tests, samples were prepared by drop casting LDHs or palladium LDH heterostructures from an aqueous dispersion onto 1×1 in² binder-free borosilicate glass microfiber filters (Whatman, GF/F, 0.7 μm). The gas phase photocatalytic measurements were conducted in a custom-built 1.5 mL stainless steel batch reactor with a fused silica view port sealed with a Viton O-ring. The reactor was evacuated using an Alcatel dry pump prior to being purged with hydrogen gas (99.9995%) at a flow rate of 6 mL min⁻¹. After purging, the reactor was infiltrated with hydrogen and carbon dioxide gas at a 4:1 ratio. The pressure inside the reactor was monitored during the reaction using an Omega PX309 pressure transducer. During purging, the reactors were heated to the desired temperature and sealed once reached. The reactor temperatures were controlled by an OMEGA CN616 6-Zone temperature controller combined with a thermocouple placed in contact with the sample. The samples were irradiated with a 1000 W Hortilux Blue metal halide bulb and continued for a period of 14–17 h. Product gases were analyzed with a flame ionization detector (FID) and thermal conductivity detector (TCD) installed in a SRI-8610 gas chromatograph (GC) with a 3' Mole Sieve 13a and 6' Haysep D column.

Isotope tracing experiments were performed using ¹³CO₂ (99.9 atomic% Sigma Aldrich). The reactors were evacuated prior to being injected with 7 psi = 0.05 MPa of ¹³CO₂ and 28 psi = 0.19 MPa of hydrogen gas to reach a final testing pressure of 35 psi = 0.24 MPa. Isotope product gases were measured using an Agilent 7890 A GC-MS with a 60 m GS-Carbon plot column fed to the mass spectrometer.

Acknowledgements

DS and MG gratefully acknowledge the funding provided by the American University of Beirut Research Board and by the Lebanese National Council for Scientific Research (LCNSR). MH acknowledges the funding provided by the Masri institute at AUB (#102882). The authors are grateful to Professor Geoffrey A. Ozin laboratory at University of Toronto for providing access to their gas phase photoreactors setup. We also thank Miss Jia Jia, Abdi-noor Jelle, and Mr. Kristian Elchami at GAO group for their assistance in the photocatalytic tests.

Keywords: cadmium/aluminum · carbon dioxide · layered double hydroxide · photoreduction · reaction diffusion framework

- [1] C. Li, M. Wei, D. G. Evans, X. Duan, *Small* **2014**, *10*, 4469–4486.
- [2] Y. Zhao, S. Zhang, B. Li, H. Yan, S. He, L. Tian, et al., *Chem. Eur. J.* **2011**, *17*, 13175–13181.
- [3] J. S. Valente, F. Tzompantzi, J. Prince, J. G. Cortez, R. Gomez, *Appl. Catal. B* **2009**, *90*, 330–338.
- [4] V. Rives, *Layered double hydroxides: present and future*, Nova Publishers, **2001**.
- [5] Q. Wang, D. O'Hare, *Chem. Rev.* **2012**, *112*, 4124–4155.
- [6] F. Cavani, F. Trifirò, A. Vaccari, *Catal. Today* **1991**, *11*, 173–301.
- [7] A. I. Khan, D. O'Hare, *J. Mater. Chem.* **2002**, *12*, 3191–3198.
- [8] J. L. Suter, R. L. Anderson, H. C. Greenwell, P. V. Coveney, *J. Mater. Chem.* **2009**, *19*, 2482–2493.
- [9] M.-A. Thyveetil, P. V. Coveney, H. C. Greenwell, J. L. Suter, *J. Am. Chem. Soc.* **2008**, *130*, 4742–4756.
- [10] P. Padma Kumar, A. G. Kalinichev, R. J. Kirkpatrick, *J. Phys. Chem. B* **2006**, *110*, 3841–3844.
- [11] P. P. Kumar, A. G. Kalinichev, R. J. Kirkpatrick, *J. Phys. Chem. C* **2007**, *111*, 13517–13523.
- [12] K. Teramura, S. Iguchi, Y. Mizuno, T. Shishido, T. Tanaka, *Angew. Chem.* **2012**, *124*, 8132–8135.
- [13] G. Fan, F. Li, D. G. Evans, X. Duan, *Chem. Soc. Rev.* **2014**, *43*, 7040–7066.
- [14] K. Parida, L. Mohapatra, *Dalton Trans.* **2012**, *41*, 1173–1178.
- [15] N. Ahmed, Y. Shibata, T. Taniguchi, Y. Izumi, *J. Catal.* **2011**, *279*, 123–135.
- [16] N. Ahmed, M. Morikawa, Y. Izumi, *Catal. Today* **2012**, *185*, 263–269.
- [17] J. Rahbani, N. M. Khashab, D. Patra, M. Al-Ghoul, *J. Mater. Chem.* **2012**, *22*, 16361–16369.
- [18] J. Rahbani, A. R. Behzad, N. M. Khashab, Al-M. Ghoul, *Electrophoresis* **2013**, *34*, 405–408.
- [19] S. P. Newman, W. Jones, *J. New Chem.* **1998**, *22*, 105–115.
- [20] B. Li, J. He, *J. Phys. Chem. C* **2008**, *112*, 10909–10917.
- [21] Y. Kuang, L. Zhao, S. Zhang, F. Zhang, M. Dong, S. Xu, *Materials* **2010**, *3*, 5220–5235.
- [22] P. J. Haines, *Thermal methods of analysis: principles, applications and problems*, Springer Science & Business Media, **2012**.
- [23] M. D. Jackson, J. Moon, E. Gotti, R. Taylor, S. R. Chae, M. Kunz, A.-H. Emwas, C. Meral, P. Guttmann, P. Levitz, H.-R. Wenk, P. J. M. Monteiro, *J. Am. Ceram. Soc.* **2013**, *96*, 2598–2606.
- [24] S. Lowell, J. E. Shields, M. A. Thomas, M. Thommes, *Characterization of porous solids and powders: surface area, pore size and density*, Springer Science & Business Media, **2012**.
- [25] S. Lowell, J. E. Shields, *Powder surface area and porosity*, Springer Science & Business Media, **2013**.
- [26] L. B. Hoch, T. E. Wood, P. G. O'Brien, K. Liao, L. M. Reyes, C. A. Mims, et al., *Adv. Sci.* **2014**, *1*, 1400013.
- [27] O'Brien P. G., Sandhel A., Wood T. E., Jelle A. A., Hoch L. B., Perovic D. D., et al., *Adv. Sci.* **2014**, *1*, 1400001.
- [28] We attempted to perform the photocatalytic reactions with a shorter reaction duration (i.e., 2–3 h); however, the amount of the ¹³CO product was too small to be detected by GC–MS.
- [29] J. Hong, W. Zhang, Y. Wang, T. Zhou, R. Xu, *ChemCatChem* **2014**, *6*, 2315–2321.
- [30] M. Hmadeh, V. Hoepfner, E. Larios, K. Liao, J. Jia, Jose-M. Yacaman, et al., *ChemSusChem* **2014**, *7*, 2104–2109.
- [31] J. R. Kremer, D. N. Mastrorarde, J. R. McIntosh, *J. Struct. Biol.* **1996**, *116*, 71–76.
- [32] D. N. Mastrorarde, *J. Struct. Biol.* **1997**, *120*, 343–352.

Received: January 21, 2016

Published online on March 29, 2016